10-15-2010

Tilted guides with friction in web conveyance systems

M. R. Brake
Sandia National Laboratories

Jonathan A. Wickert
Iowa State University, wickert@iastate.edu

Tilted guides with friction in web conveyance systems

Abstract
One challenge in designing web conveyance systems is controlling the displacement and vibration of the webs by guides without introducing instabilities or higher frequency disturbances from flange impacts. A solution to this problem is to use an actively or passively tilted guide or roller to steer the web. In this paper, a model of tilted guides with friction is developed, and it is shown that tilted guides produce a change in the web's displacement, slope, bending moment, and shear force. When the web is conceptually unwrapped from its path, the normal force between the web and a tilted guide has a component that acts in the direction of the web's lateral displacement, resulting in an equivalent force and bending moment acting on the web. The model is validated by measurements, and is compared to a previously existing model of guide tilt. In the configurations studied, the displacement of the web near the guide is linearly dependent on the tilt angle and tension and it increases exponentially with the web's span length. When the guide's tilt is oriented towards the center of the web's wrap around the guide, the equivalent bending moment is zero in the absence of friction, and there is good agreement between the model developed in this paper and the previously existing model. However, when the center of the web's wrap is oriented 90° away from the guide's tilt orientation, the equivalent force is zero in the absence of friction, and measurements demonstrate the necessity of the equivalent bending moment.

Disciplines
Mechanical Engineering

Comments
This article is from *International Journal of Solids and Structures* 47 (2010): 2952–2957, doi:10.1016/j.ijsolstr.2010.06.019.

International Journal of Solids and Structures 47 (2010) 2952–2957

Contents lists available at ScienceDirect

International Journal of Solids and Structures

journal homepage: www.elsevier.com/locate/ijsolstr

Tilted guides with friction in web conveyance systems

M.R. Brake [a,*], J.A. Wickert [b]

[a] Applied Mechanics Development Department, Sandia National Laboratories,[1] Albuquerque, NM 87185, United States
[b] Department of Mechanical Engineering, Iowa State University, Ames, IA 50011, United States

ARTICLE INFO

Article history:
Received 13 April 2009
Available online 23 July 2010

Keywords:
Webs
Magnetic tape
Tilt
Tilted guides
Friction

ABSTRACT

One challenge in designing web conveyance systems is controlling the displacement and vibration of the webs by guides without introducing instabilities or higher frequency disturbances from flange impacts. A solution to this problem is to use an actively or passively tilted guide or roller to steer the web. In this paper, a model of tilted guides with friction is developed, and it is shown that tilted guides produce a change in the web's displacement, slope, bending moment, and shear force. When the web is conceptually unwrapped from its path, the normal force between the web and a tilted guide has a component that acts in the direction of the web's lateral displacement, resulting in an equivalent force and bending moment acting on the web. The model is validated by measurements, and is compared to a previously existing model of guide tilt. In the configurations studied, the displacement of the web near the guide is linearly dependent on the tilt angle and tension and it increases exponentially with the web's span length. When the guide's tilt is oriented towards the center of the web's wrap around the guide, the equivalent bending moment is zero in the absence of friction, and there is good agreement between the model developed in this paper and the previously existing model. However, when the center of the web's wrap is oriented 90° away from the guide's tilt orientation, the equivalent force is zero in the absence of friction, and measurements demonstrate the necessity of the equivalent bending moment.

Published by Elsevier Ltd.

1. Introduction

The mitigation and control of the lateral vibration of axially-moving materials is a key problem affecting the magnetic tape, automotive belt drive, conveyor belt, polymer web, sheet metal, and paper processing industries. Models of the displacement and vibration of axially-moving materials (Wickert and Mote, 1988; Young and Reid, 1993), termed webs, include traveling strings (Chen, 2005) and membranes (Shin et al., 2004), and traveling tensioned beams (Wickert and Mote, 1990) and plates (Lin, 1997). The web itself travels over a series of guides and rollers that are used to both constrain its lateral motion and position the web in its path.

Solutions to passively control the displacement of the web include the use of flanged edge guides and surface guides. Edge guides use rigid or compliant flanges to apply lateral forces to the narrow edge of the web to constrain lateral vibration. The judicious design and placement of edge guides along the path can significantly reduce the steady-state vibration amplitude (Kartik and Wickert, 2006; Chakraborty and Mallik, 1999); however, contact between the webs and the guide's flanges can excite high frequency vibration (Boyle and Bhushan, 2006). Non-uniform or asymmetric edge loading via the flanges can even lead to the web wrinkling (Kim, 2009). In surface guiding, edge contact is avoided entirely, and lateral vibration is controlled by distributing friction forces over the relatively broad face of the web's width (Ono, 1979). This approach is particularly effective at mitigating high frequency vibration (Kartik and Wickert, 2007); however, in some applications it can exacerbate the disturbances (Cheng and Zu, 2003). Dry friction guides are associated with the instability of moving string models at supercritical speeds (Cheng and Perkins, 1991; Chen, 1997), and the instability range extends to subcritical speeds (Zen and Müftü, 2006) with axial acceleration.

An alternative approach to control the displacement of the axially-moving materials is to use a tilted roller or guide. A web winding around a tilted roller is modeled in Shelton and Reid (1971a,b) with a kinematic boundary condition that matches the velocity of the web to the velocity of the roller. Extensions of this method focus on adapting it to higher order models (Benson, 2002) and controlling the lateral position of a web by actively tilting or laterally displacing rollers (Sievers et al., 1988; Yerashunas et al., 2003; Shin and Kwon, 2007). The effect of tilting a smooth tilted post on the displacement of a beam is developed in Eaton (1998). This model shows that a smooth tilted post with a stationary beam wrapped around it affects the beam's displacement, slope, and shear force. Models and an experiment using an actuator

* Corresponding author. Tel.: +1 505 284 3351.
E-mail address: mrbrake@sandia.gov (M.R. Brake).

[1] Sandia is a multiprogram laboratory operated by Sandia Corporation, a Lockheed Martin Company, for the United States Department of Energy's National Nuclear Security Administration under Contract DE-AC04-94-AL85000.

0020-7683/$ - see front matter Published by Elsevier Ltd.
doi:10.1016/j.ijsolstr.2010.06.019

that produces a change in a traveling string's displacement, slope, bending moment, and shear force are shown to be effective in attenuating the vibration of the string (de Queiroz et al., 1999; Nagarkatti et al., 2002), and the efficacy of using an actively tilted guide to steer an axially-moving material is demonstrated in Xia et al. (2005).

In what follows in Section 2, a new model of guide tilt is developed that incorporates friction at the interface between the guide and the web. It is found that in addition to the tilted guide producing a change in the web's displacement, slope, and shear force, there is an additional change in the web's bending moment, even in the absence of friction. While the present model and (Eaton, 1998) are similar in several aspects for the case of a smooth, frictionless, tilted post, the differences are highlighted in a validation study presented in Section 3, which demonstrates the necessity of including the change in the material's bending moment.

2. Guide tilt model

The web is conceptually unwrapped from its path and modeled as having displacement z in the lateral direction (the x_3 direction in Fig. 1), transport speed v, and tension T that extends from $x = 0$ to L in the global axial coordinate system. A guide is located at an arbitrary position along the path such that its surface is first contacted by the web at $x = L_1$, and has friction coefficient μ, radius r, and wrap angle $\theta_2 - \theta_1$, where the positions along the guide at which the web first contacts it and the web loses contact are denoted θ_1 and θ_2. Although tension T is constant in each free span, it increases from T_0 at θ_1 along the guide's circumference following:

$$T(\theta) = T_0 e^{\mu(\theta-\theta_1)}. \tag{1}$$

The effect of friction on the web's lateral motion is further discussed in Ono (1979), Kartik and Wickert (2007), Brake and Wickert (2008).

In Fig. 1(a), a cylindrical guide is tilted an angle δ from the global x_3 axis, which is orthogonal to the system's global $x_1 - x_2$ datum plane. The guide's orientation is defined such that the projections of the guide's local $x_1^{(1)}$ and $x_3^{(1)}$ axes onto the $x_1 - x_2$ plane are coincident, while the local $x_2^{(1)}$ axis lies in the $x_1 - x_2$ plane. The guide's local coordinates are related to the global coordinates by the tilt orientation angle α, and the position along the guide θ is defined relative to the $x_1^{(1)}$ axis, as shown in Fig. 2(a). A disc formed from the cross-section of the guide (Fig. 1(b)) has height

$$h(\theta) = -r\sin(\delta)\cos(\theta), \tag{2}$$

from the $x_1 - x_2$ plane and has position along its edge $s = Jr\theta$, with $J = 1$ for counter-clockwise wrapping of the web and -1 for clockwise wrapping. The web wraps around the guide with a helix angle ψ (Fig. 2(b)) and has engagement length

$$s_p = \frac{Jr(\theta_2 - \theta_1)}{\cos(\psi)}. \tag{3}$$

The tilted guide produces a change in displacement z of the web

$$\begin{aligned} z_\delta &= h(\theta_2) - h(\theta_1) + \int_{\theta_1}^{\theta_2} Jr\tan(\psi)d\theta \\ &= -r\sin(\delta)(\cos(\theta_2) - \cos(\theta_1)) + Jr(\theta_2 - \theta_1)\tan(\psi), \end{aligned} \tag{4}$$

and a change in slope

$$\phi_\delta = \left.\frac{dh}{ds}\right|_{\theta_1}^{\theta_2} = J\sin(\delta)(\sin(\theta_2) - \sin(\theta_1)). \tag{5}$$

The slope of the web ϕ over the guide with respect to the global coordinates is related to the helix angle ψ through

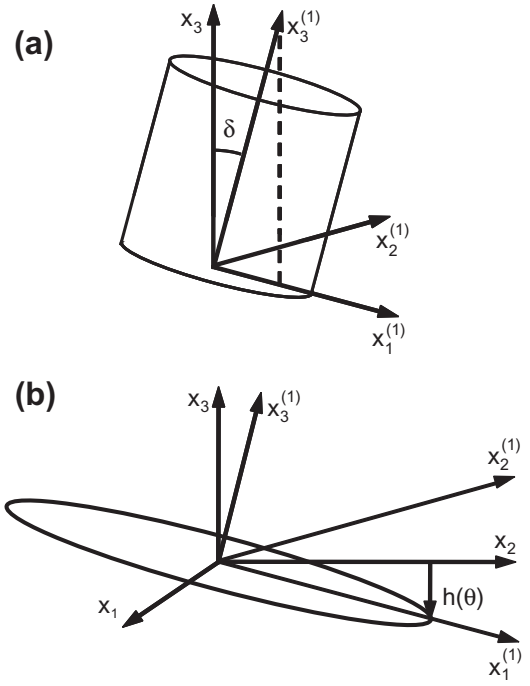

Fig. 1. (a) Definition of the tilt angle δ and (b) definition of the tilted cross section's height $h(\theta)$.

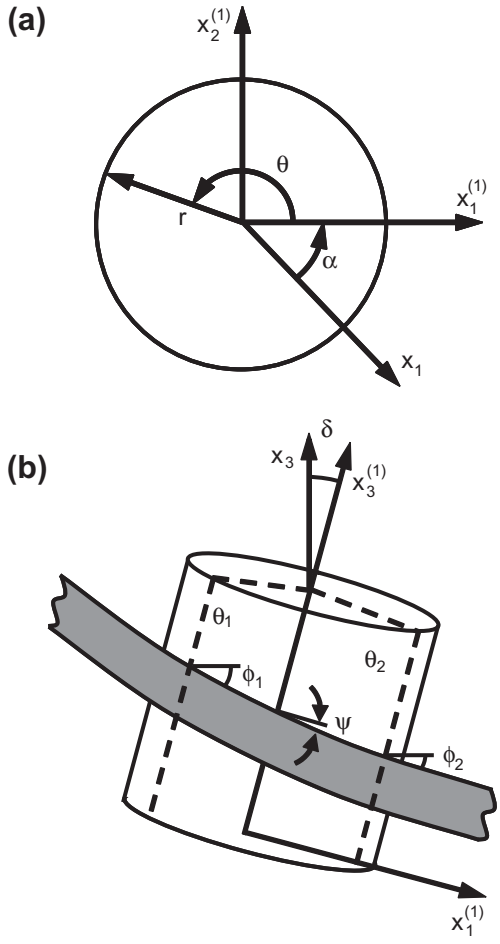

Fig. 2. (a) Relation of the global coordinates x_1 and x_2 to the local coordinates $x_1^{(1)}$ and $x_2^{(1)}$ by the orientation angle α, and (b) definition of the inlet slope ϕ_1 at θ_1 and the outlet slope ϕ_2 at θ_2 with respect to the global coordinate system, and the helix angle ψ defined relative to the local coordinate system.

$$\phi(\theta) = \left.\frac{dh}{ds}\right|_{\theta} + \psi. \tag{6}$$

In the web transport systems considered, both ψ and ϕ are small such that $\tan(\psi) \approx \psi$ in Eq. (4).

While the normal force per unit of length $N(\theta) = T(\theta)/r$ acts perpendicular to the guide's surface, it has a component that is resolved in the x_3 direction as shown in Fig. 3. Integration of the lateral component of the normal force yields an equivalent force and bending moment that acts on the unwrapped web at $(\theta_1 + \theta_2)/2$

$$\begin{aligned} F_\delta &= \int_{\theta_1}^{\theta_2} -N(\theta)\sin(\delta)\cos(\theta) r d\theta \\ &= -\frac{T_0 \sin(\delta)}{\mu^2+1}\left(e^{\mu(\theta_2-\theta_1)}(\mu\cos(\theta_2)+\sin(\theta_2)) \right. \\ &\quad \left. -(\mu\cos(\theta_1)+\sin(\theta_1))\right) \end{aligned} \tag{7}$$

$$\begin{aligned} M_\delta &= \int_{\theta_1}^{\theta_2} F(\theta)\left(\frac{\theta_2+\theta_1}{2}-\theta\right) r^2 d\theta \\ &= -\frac{T_0 r \sin(\delta)}{\mu^2+1}\left(e^{\mu(\theta_2-\theta_1)}\left(\left(\mu\frac{\theta_1-\theta_2}{2}+\frac{\mu^2-1}{\mu^2+1}\right)\cos(\theta_2)\right.\right. \\ &\quad \left.-\left(\frac{\theta_2-\theta_1}{2}-\frac{2\mu}{\mu^2+1}\right)\sin(\theta_2)\right) \\ &\quad \left.-\left(\left(\mu\frac{\theta_2-\theta_1}{2}+\frac{\mu^2-1}{\mu^2+1}\right)\cos(\theta_1)-\left(\frac{\theta_1-\theta_2}{2}-\frac{2\mu}{\mu^2+1}\right)\sin(\theta_1)\right)\right). \end{aligned} \tag{8}$$

For the case of no friction, F_δ and M_δ simplify to

$$F_\delta = -T_0 \sin(\delta)(\sin(\theta_2) - \sin(\theta_1)) \tag{9}$$

$$M_\delta = T_0 r \sin(\delta)\left(\frac{\theta_2-\theta_1}{2}(\sin(\theta_2)+\sin(\theta_1)) + \cos(\theta_2) - \cos(\theta_1)\right). \tag{10}$$

The results (2)–(5) and (9) agree with the derivation of Eaton (1998) for the case of no friction; however, the present analysis concludes that there is also an equivalent bending moment (8) that acts on the web.

For a guide with an arbitrary force–deflection constitutive relationship $F_G(z)$ acting at the center of the wrap length, guide tilt changes the reference datum of the guide by a height $h((\theta_1 + \theta_2)/2)$. In the simple case of a linear, compliant guide of stiffness K, the force–deflection relationship is $F_G = Kz$ for a guide without tilt. In the presence of tilt, the force–deflection constitutive relationship becomes

$$F_G = K\left(z - h\left(\frac{\theta_1+\theta_2}{2}\right)\right) = K\left(z + r\sin(\delta)\cos\left(\frac{\theta_1+\theta_2}{2}\right)\right). \tag{11}$$

3. Validation study

The test stand shown in Fig. 4 is used to validate the tilted guide model. A pressurized air bearing guide, which has $\mu = 0$ due to an air bearing between the guide and the web, is mounted to a fixed axis rotation stage termed a goniometer. An adapter plate fixes the guide such that the center of the guide's surface is coincident with the center of the goniometer's axis of rotation. Clamped-free specimens of magnetic tape are mounted in three different configurations that vary the wrap angle $\theta_2 - \theta_1$. The clamped end is fixed

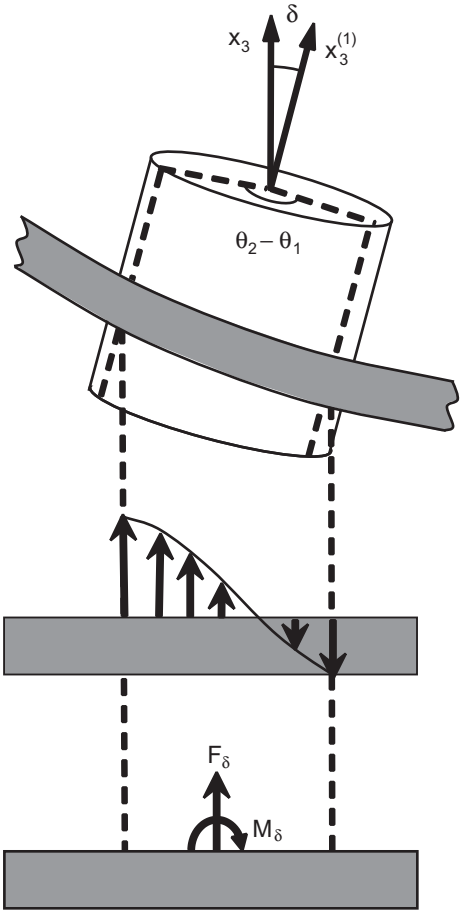

Fig. 3. The normal force $N(\theta)$ between the guide and the web has lateral component $N(\theta)\sin(\delta)\cos(\theta)$, which can be expressed as an equivalent force F_δ and moment M_δ acting on the unwrapped tape.

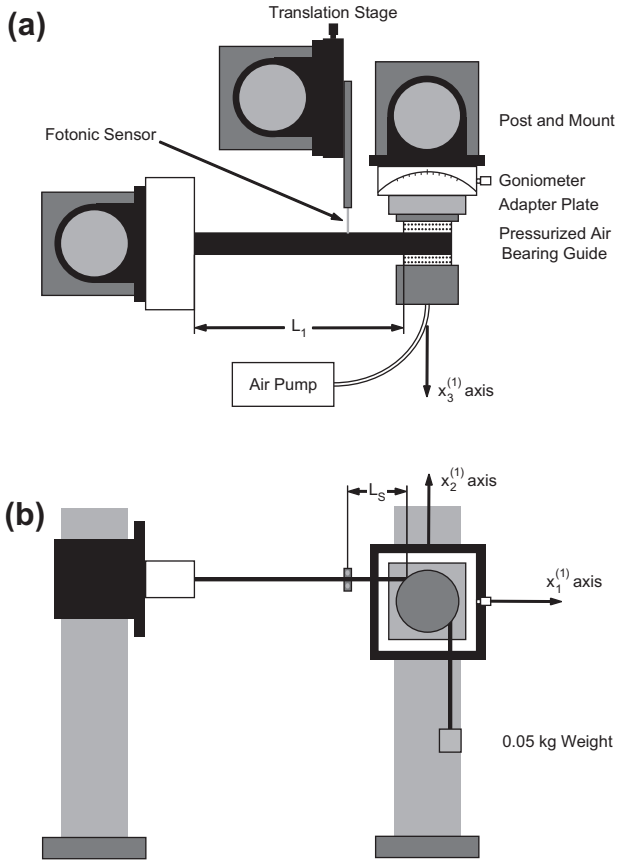

Fig. 4. The test stand used in the model validation study in the first configuration, viewed from (a) above and (b) the side.

with epoxy between two blocks, and the free end has a 0.05 kg mass attached to it. The displacement of the web is measured at a distance L_S from the inlet of the guide with an MTI Fotonic sensor. Material properties and lengths of the specimen and parameters for the test stand are listed in Table 1.

The deflection of the web is calculated using a static Euler-Bernouli model for a clamped-free, tensioned beam divided into two sections $x \in (0, L_1)$ and $x \in (L_1 + L_R, L)$

$$EIz'''' - Tz'' = 0 \tag{12}$$

$$\begin{aligned} &z(0) = 0 \quad z'(0) = 0 \\ &z(L_1) - z(L_1 + L_R) = -z_\delta \quad z'(L_1) - z'(L_1 + L_R) = -\phi_\delta \\ &z''(L_1) - z''(L_1 + L_R) = \frac{-M_\delta}{EI} \quad z'''(L_1) - z'''(L_1 + L_R) = \frac{F_\delta}{EI} \\ &z''(L) = 0 \quad z'''(L) = 0, \end{aligned} \tag{13}$$

where $(\bullet)'$ indicates differentiation with respect to the global axial coordinate x and $L_R = r(\theta_2 - \theta_1)$ is the wrap length. The solution in each span j is of the form

$$z(x) = \gamma_{j1} e^{\sqrt{\frac{T}{EI}}x} + \gamma_{j2} e^{-\sqrt{\frac{T}{EI}}x} + \gamma_{j3} x + \gamma_{j4}, \tag{14}$$

with coefficients $\gamma_{j1} - \gamma_{j4}$ that are solved simultaneously using the boundary conditions of Eq. (13). Over the guide $x \in [L_1, L_1 + L_R]$, the web is wrapped in a helix with displacement

$$\begin{aligned} z(x) &= z(L_1) + h(\theta(x)) - h(\theta_1) + \int_{\theta_1}^{\theta(x)} Jr \tan(\psi) d\theta \\ &= z(L_1 - L_R) - r\sin(\delta)(\cos(\theta(x)) - \cos(\theta_1)) \\ &\quad + Jr(\theta(x) - \theta_1)\left(\left.\frac{dz}{dx}\right|_{L_1 - L_R} - J\sin(\delta)\sin(\theta_1)\right), \end{aligned} \tag{15}$$

and has angular position $\theta(x) = (x - L_1)/r + \theta_1$. For comparison, the same solution technique is used to find the displacement predicted by Eaton (1998).

In the first configuration (shown in Fig. 4), the web has a wrap angle of 90°. The tilt angle δ is varied from 0 to 9.1 mrad for two different lengths of tape ($L = 0.285$ m in Fig. 5(a) and 0.500 m in Fig. 5(b)). The displacement of the web at $x = L_1 - L_S$ increases linearly with δ for both lengths, and as the length is increased, the displacement of the web at the sensor position is likewise increased. At this scale for this configuration, there is no appreciable difference between the present model and (Eaton, 1998). The effect of the first span's length L_1 on the web's displacement, with L held constant, is reported in Fig. 6 for the first configuration. The displacement increases exponentially with L_1, suggesting that proper selection of span lengths is just as important as the tilt angle for passively controlling the web's displacement. In this configuration, there is a 3.8% difference at $L_1 = 0.15$ m between the two models, with measurements equally supporting both models. Likewise, as the tension is varied in Fig. 7 for the first configuration, the displacement of the web increases linearly with a 3.5% difference between the two models for $T = 0.5$ N. In these cases, there is good agreement between the experimental data and both models since the contribution of M_δ in the first configuration is small compared to F_δ.

Table 1
Parameters for the validation study.

Parameter	Value
Bending stiffness, EI	9.988 mN m ^{2}
Coefficient of friction, μ	0
Guide radius, r	15.85 mm
Tension, T	0.5 N
Specimen 1	
Span 1 length, L_1	0.157 m
Total length, L	0.285 m
Specimen 2	
Span 1 length, L_1	0.395 m
Total length, L	0.500 m
Specimen 3	
Span 1 length, L_1	0.076 m
Total length, L	0.254 m
Test stand configuration 1	
Inlet angle, θ_1	− 90°
Outlet angle, θ_2	0°
Sensor position, L_S	0.050 m
Test stand configuration 2	
Inlet angle, θ_1	0°
Outlet angle, θ_2	180°
Sensor position, L_S	0.050 m
Test stand configuration 3	
Inlet angle, θ_1	− 30°
Outlet angle, θ_2	0°
Sensor position, L_S	0.040 m

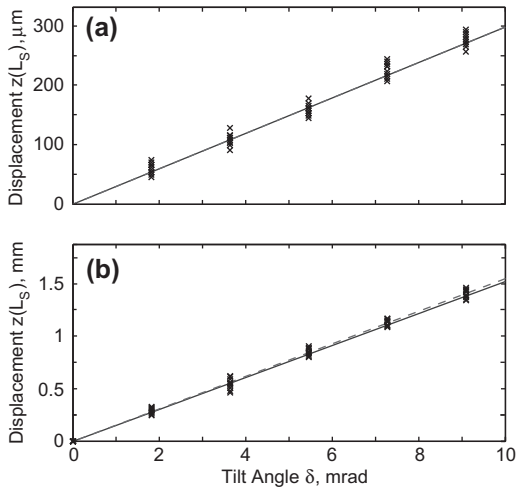

Fig. 5. Displacement of the web as a function of the tilt angle δ for the first configuration with (a) $L = 0.285$ m and $L_1 = 0.157$ m, and (b) $L = 0.500$ m and $L_1 = 0.395$ m. The present model (—), (Eaton, 1998) (----), and measured values (×) are shown; $\theta_2 - \theta_1 = 90°$, $\alpha = 45°$, and $L_S = 0.050$ m.

In the second configuration, the web has a wrap angle of 180°, the tilt angle is varied from 0 to 9.1 mrad for two different specimen lengths ($L = 0.285$ m in Fig. 8(a) and 0.500 m in Fig. 8(b)), and the displacement of the web is measured at $x = L_1 - L_S$. Similar to the first configuration, as the length is increased the displacement of the web at the sensor position is also increased, and the

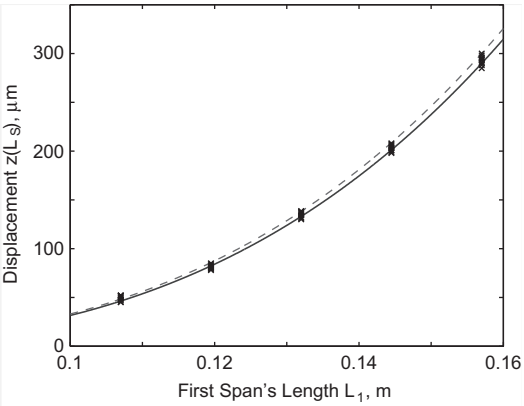

Fig. 6. Displacement of the web as a function of the first span's length L_1 in the first configuration for the present model (—), (Eaton, 1998) (----), and measured values (×); $\theta_2 - \theta_1 = 90°$, $\alpha = 45°$, $L_S = 0.050$ m, $L = 0.285$ m, and $\delta = 9.09$ mrad.

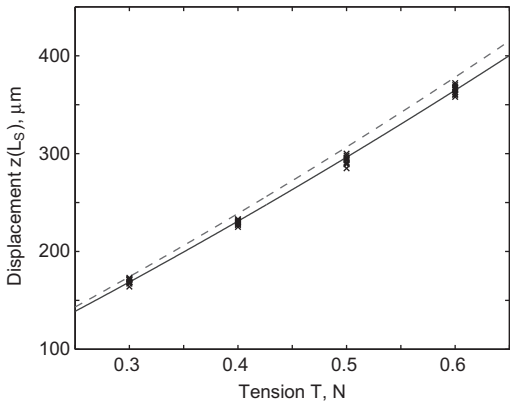

Fig. 7. Displacement of the web as a function of the web's tension T in the first configuration for the present model (—), (Eaton, 1998) (----), and measured values (×); $\theta_2 - \theta_1 = 90°$, $\alpha = 45°$, $L = 0.285$ m, $L_S = 0.050$ m, $L_1 = 0.157$ m, and $\delta = 9.09$ mrad.

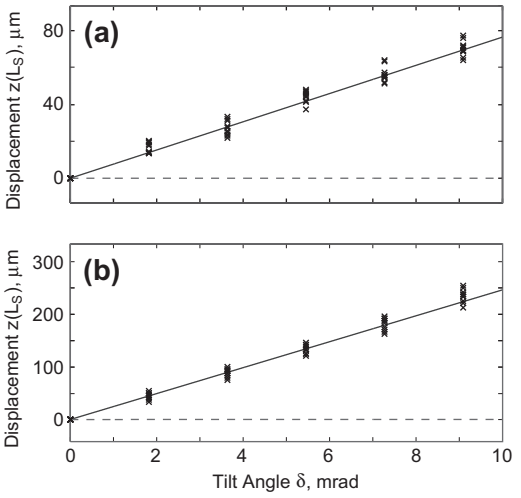

Fig. 8. Displacement of the web as a function of the tilt angle δ for the second configuration with (a) $L = 0.285$ m and $L_1 = 0.157$ m, and (b) $L = 0.500$ m and $L_1 = 0.395$ m. The present model (—), (Eaton, 1998) (----), and measured values (×) are shown; $\theta_2 - \theta_1 = 180°$, $\alpha = 0°$, and $L_S = 0.050$ m.

web's displacement linearly increases with δ. There is good agreement between the present model and the data; however, because (Eaton, 1998) does not consider the equivalent bending moment, it predicts negligible displacement at the sensor location for all δ.

The orientation angle α of the tilt axis (measured counter-clockwise from the $x_1^{(1)}$ axis shown in Fig. 4) is varied in Fig. 9(a) for the first configuration and in Fig. 9(b) for the second configuration. When the center of the wrap angle $\beta = (\theta_2 + \theta_1)/2 = 90°$ (at $\alpha = -45°$ in Fig. 9(a) and 0° in Fig. 9(b)), (Eaton, 1998) predicts no displacement while the present model predicts-15 and 66 μm for the first and second configurations respectively. This result holds even for small span lengths and wrap angles, as shown in Fig. 10 for the third test stand configuration and third specimen. Fig. 11 shows that the contribution of M_δ to the web's displacement is most significant for β near ± 90° and for large wrap angles. The relative contribution of the moment term with respect to the force term

$$\eta = \left| \frac{z(L_S) - z_E(L_S)}{z_E(L_S)} \right|, \tag{16}$$

where z_E is the displacement calculated from Eaton (1998), increases as the wrap angle $\theta_2 - \theta_1$ is increased. For $\theta_2 - \theta_1 = 180°$, $\eta > 0.1$ over 64% of $\beta \in (-180°, 180°)$, and $\eta > 1$ for 10% of β.

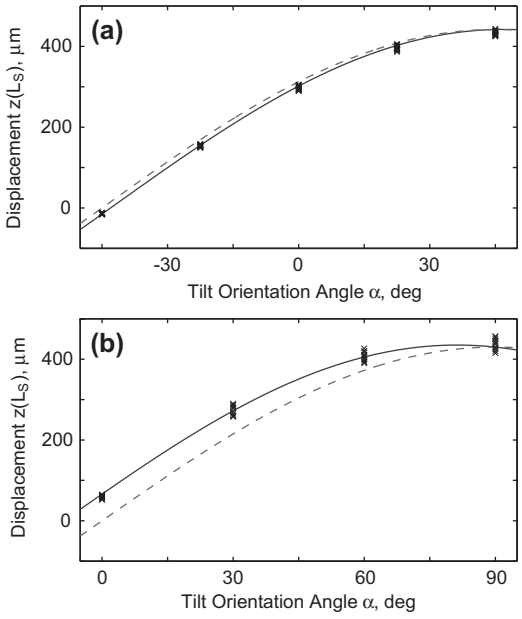

Fig. 9. Displacement of the web as a function of the tilt orientation angle α for (a) the first configuration with a 90° wrap angle and (b) the second configuration with a 180° wrap angle. The present model (—), (Eaton, 1998) (----), and measured values (×) are shown; $L = 0.285$ m, $L_1 = 0.157$ m, and $\delta = 9.09$ mrad.

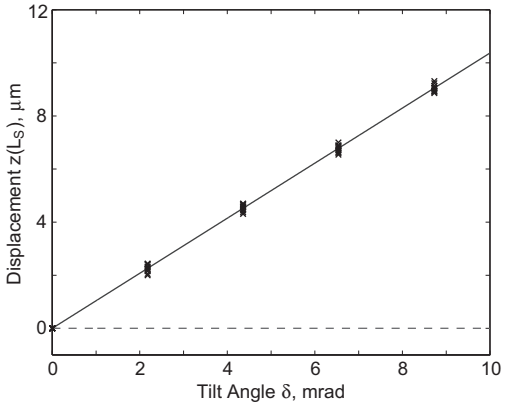

Fig. 10. Displacement of the web as a function of the tilt angle δ for the third configuration. The present model (—), (Eaton, 1998) (----), and measured values (×) are shown; $\theta_2 - \theta_1 = 30°$, $\gamma = 90°$, $L = 0.254$ m, $L_1 = 0.076$ m, and $L_S = 0.040$ m.

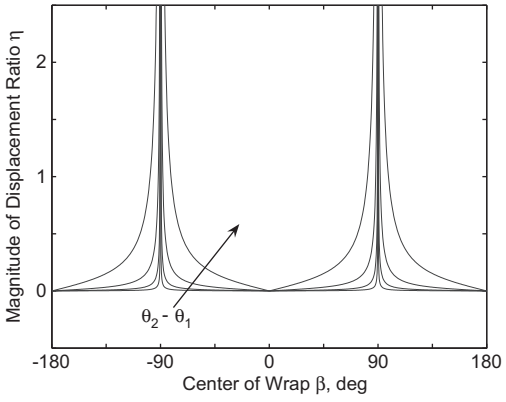

Fig. 11. Relative contribution η of the bending moment term to the shear force term as a function of the center of the wrap angle β for wrap angles $\theta_2 - \theta_1 = 30, 60, 90$, and 180°; $\mu = 0$, $L = 0.254$ m, $L_1 = 0.076$ m, $L_S = 0.040$, and $\delta = 9.09$ mrad.

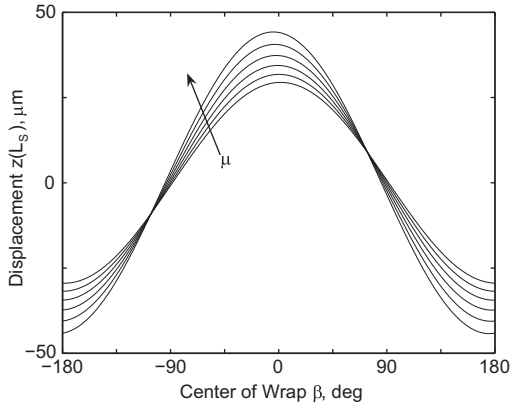

Fig. 12. Displacement of the web as a function of the center of the wrap angle β for coefficients of friction $\mu = 0, 0.1, 0.2, 0.3, 0.4$, and 0.5; $L = 0.285$ m, $L_1 = 0.157$ m, $L_s = 0.080$, $\theta_2 - \theta_1 = 90°$, and $\delta = 9.09$ mrad.

The effect of friction on the displacement of the web is shown in Fig. 12 for $\theta_2 - \theta_1 = 90°$. As μ is increased, the displacement with respect to β becomes skew symmetric because of the friction increasing exponentially along the length of the guide. Away from $\beta \in [-105, -90]$ and [75,90], the magnitude of the web's displacement increases with μ. The point at which the displacement of the responses coincides is shifted 15° from ±90° by the presence of friction in this configuration.

4. Summary

A model of guide tilt with friction and arbitrary force–deflection constitutive relationship is developed in order to calculate the change in displacement, slope, bending moment, and shear force for a web wrapped around a tilted guide. The model is validated for the case of a frictionless post by measurements and is compared to the previously existing model (Eaton, 1998) of guide tilt. The primary conclusions and contributions are:

1. The normal force between a web and a tilted guide has a component that acts in the direction of the web's lateral displacement, resulting in an equivalent force and bending moment acting on the web.
2. The displacement of the web at a position near a tilted guide is linearly dependent on the guide's tilt angle (for small tilt angles) and the web's tension and is shown to increase exponentially with the web's span length.
3. When the guide's tilt is oriented towards the center of the web's wrap around the guide, the equivalent bending moment is zero in the absence of friction and there is good agreement between the present model and (Eaton, 1998).
4. When the center of the wrap is oriented 90° away from the guide's tilt orientation, the equivalent force is zero in the absence of friction, and measurements demonstrate the necessity of the equivalent bending moment term.

Acknowledgements

The authors gratefully acknowledge the support and collaboration from the Information Storage Industry Consortium and the assistance provided by Doug Johnson of Imation Corporation. The authors would also like to thank Carnegie Mellon University's Department of Mechanical Engineering, where this research was conducted, and Prof. Bill Messner for his feedback on drafts of this paper.

References

Benson, R.C., 2002. Lateral dynamics of a moving web with geometrical imperfection. ASME Journal of Dynamic Systems, Measurement, and Control 124, 25–34.
Boyle, J.M., Bhushan, B., 2006. Vibration modeling of magnetic tape with vibro-impact of tape-guide contact. Journal of Sound and Vibration 289, 632–655.
Brake, M.R., Wickert, J.A., 2008. Frictional vibration transmission from a laterally moving surface to a traveling beam. Journal of Sound and Vibration 310, 663–675.
Chakraborty, G., Mallik, A.K., 1999. Non-linear vibration of a travelling beam having an intermediate guide. Nonlinear Dynamics 20, 247–265.
Chen, J.-S., 1997. Natural frequencies and stability of an axially-traveling string in contact with a stationary load system. ASME Journal of Vibration and Acoustics 119, 152–157.
Chen, L.-Q., 2005. Analysis and control of transverse vibrations of axially moving strings. ASME Applied Mechanics Reviews 58, 91–116.
Cheng, S.-P., Perkins, N.C., 1991. The vibration and stability of a friction-guided, translating string. Journal of Sound and Vibration 144, 281–292.
Cheng, G., Zu, J.W., 2003. Nonstick and stick-slip motion of a Coulomb-damped belt drive system subjected to multifrequency excitations. ASME Journal of Applied Mechanics 70, 871–884.
de Queiroz, M.S., Dawson, D.M., Rahn, C.D., Zhang, F., 1999. Adaptive vibration control of an axially moving string. ASME Journal of Vibration and Acoustics 121, 41–49.
Eaton, J.H., 1998. Behavior of a tape path with imperfect components. Advances in Information Storage Systems 8, 77–91.
Kartik, V., Wickert, J.A., 2006. Vibration and guiding of moving media with edge weave imperfections. Journal of Sound and Vibration 291, 419–436.
Kartik, V., Wickert, J.A., 2007. Surface friction guiding for reduced high-frequency lateral vibration of moving media. ASME Journal of Vibration and Acoustics 129, 371–379.
Kim, C.H., 2009. Stress distribution and wrinkling of webs under non-uniform and asymmetric edge loading. International Journal of Solids and Structures 46, 851–859.
Lin, C.C., 1997. Stability and vibration characteristics of axially moving plates. International Journal of Solids and Structures 34, 3179–3190.
Nagarkatti, S.P., Zhang, F., Costic, B.T., Dawson, D.M., Rahn, C.D., 2002. Speed tracking and transverse vibration control of an axially accelerating web. Mechanical Systems and Signal Processing 16, 337–356.
Ono, K., 1979. Lateral motion of an axially moving string over a cylindrical guide surface. ASME Journal of Applied Mechanics 46, 905–912.
Shelton, J.J., Reid, K.N., 1971a. Lateral dynamics of an idealized moving web. ASME Journal of Dynamic Systems, Measurement, and Control 93, 187–192.
Shelton, J.J., Reid, K.N., 1971b. Lateral dynamics of a real moving web. ASME Journal of Dynamic Systems, Measurement, and Control 93, 180–186.
Shin, K.H., Kwon, S.O., 2007. The effect of tension on the lateral dynamics and control of a moving web. IEEE Transactions on Industry Applications 43, 403–411.
Shin, C., Kim, W., Chung, J., 2004. Free in-plane vibration of an axially moving membrane. Journal of Sound and Vibration 272, 137–154.
Sievers, L., Balas, M., von Flotow, A., 1988. Modeling of web conveyance systems for multivariable control. IEEE Transactions on Automatic Control 33, 524–531.
Wickert, J.A., Mote Jr., C.D., 1988. Current research on the vibration and stability of axially-moving materials. Shock and Vibration Digest 20, 3–13.
Wickert, J.A., Mote Jr., C.D., 1990. Classical vibration analysis of axially moving continua. ASME Journal of Applied Mechanics 57, 738–744.
Xia L., Messner W., Venkataraman K., Wickert J.A., 2005. Design of active steering system for reducing lateral tape motion. In : ASME 15th Conference on Information Storage and Processing Santa Clara, CA, June 27–29.
Yerashunas, J.B., Abreu-Garcia, J.A.D., Hartley, T.T., 2003. Control of lateral motion in moving webs. IEEE Transactions on Control Systems Technology 11, 684–693.
Young, G.E., Reid, K.N., 1993. Lateral and longitudinal dynamic behavior and control of moving webs. ASME Journal of Dynamic Systems, Measurement, and Control 115, 309–317.
Zen, G., Müftü, S., 2006. Stability of an axially accelerating string subjected to frictional guiding forces. Journal of Sound and Vibration 289, 551–576.